Supporting Information for

Midlatitude Oceanic Fronts Strengthen the Moisture Transport from Anticyclones to Cyclones

S. Okajima[1], H. Nakamura[1], and T. Spengler[2]

[1]Research Center for Advanced Science and Technology, The University of Tokyo, Tokyo, Japan

[2]Geophysical Institute, University of Bergen, and Bjerknes Centre for Climate Research, Bergen, Norway

Contents of this file

Introduction

The supporting information includes (1) two text sections that describe details of the JRA-55 reanalysis and how to evaluate moisture transport locally between cyclonic and anticyclonic domains, and (2) nine supplementary figures that are referred to but not presented in the main text.

Text S1.

      To verify the reproducibility of CNTL, we utilize the global atmospheric JRA-55 reanalysis (Kobayashi et al. 2015; Harada et al. 2016) in Supplementary Figs. S4 and S7 to compare the climatological-mean fields with those from CNTL. We analyze 6-hourly fields of surface sensible and latent heat fluxes as well as precipitation for the period 1958/59-2019/20. The JRA-55 has been constructed by the Japan Meteorological Agency (JMA) through a four-dimensional variational data assimilation system with TL319 horizontal resolution (equivalent to 55 km) and 60 vertical levels up to 0.1-hPa.

Harada, Y., Kamahori, H., Kobayashi, C., Endo, H., Kobayashi, S., Ota, Y., et al. (2016). The JRA-55 Reanalysis: Representation of Atmospheric Circulation and Climate Variability. *Journal of the Meteorological Society of Japan*, 94(3), 269–302.
Kobayashi, S., Ota, Y., Harada, Y., Ebita, A., Moriya, M., Onoda, H., et al. (2015). The JRA-55 Reanalysis: General specifications and basic characteristics. *Journal of the Meteorological Society of Japan*, 93(1), 5–48.

Text S2.

      As a measure of moisture transport between cyclonic and anticyclonic domains, we calculated a moisture flux projected onto the upgradient direction of local curvature. Under the assumption of a geostrophic wind balance, the upgradient direction of local curvature is normal to horizontal wind vector pointing to a larger cyclonic curvature.

      Specifically, the scaler value is evaluated at each pressure level as:

$$\epsilon \equiv (q\mathbb{v}') \cdot \frac{\nabla \kappa_2}{|\nabla \kappa_2|},$$

where $\mathbb{v}$ denotes horizontal wind, q specific humidity, κ_2 two-dimensional curvature of the wind vectors, and a prime high-pass-filtered fluctuations based on a Lanczos filter with a cutoff period of 8 days. Here, the moisture flux was calculated with high-pass-filtered wind fluctuations to measure the effectiveness of moisture transport associated with transient eddies, in analogy to (anti)cyclone-relative winds. Nevertheless, we have confirmed that a qualitatively similar result can be obtained with fluctuations calculated either with unfiltered horizontal wind components or with high-pass-filtered specific humidity. We calculated the climatological-mean value of ϵ with a mask of grid points where the local curvature radius is less than 2,500km to focus on marginal zones between cyclonic and anticyclonic domains where the moisture transport takes place. The moisture transport shown in Fig. 4 and Supplementary Fig. S8 is vertically integrated from the surface to the 100-hPa.
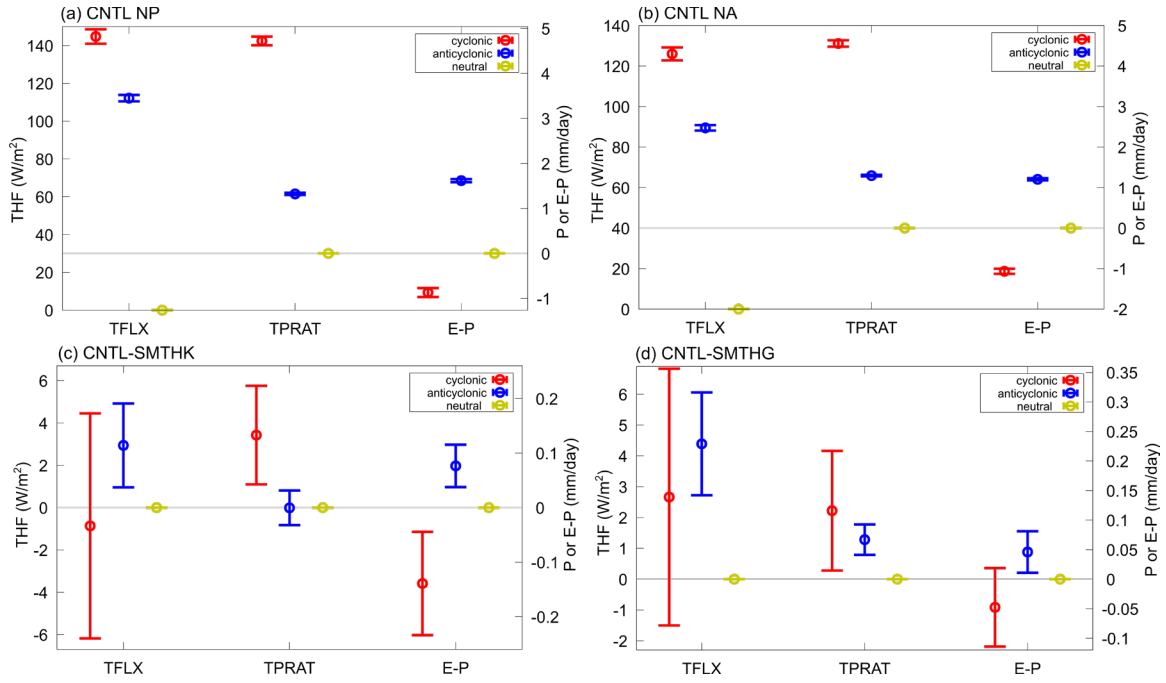
Figure S1. Same as in Fig. 3, respectively, but for the results based on a curvature threshold of zero.
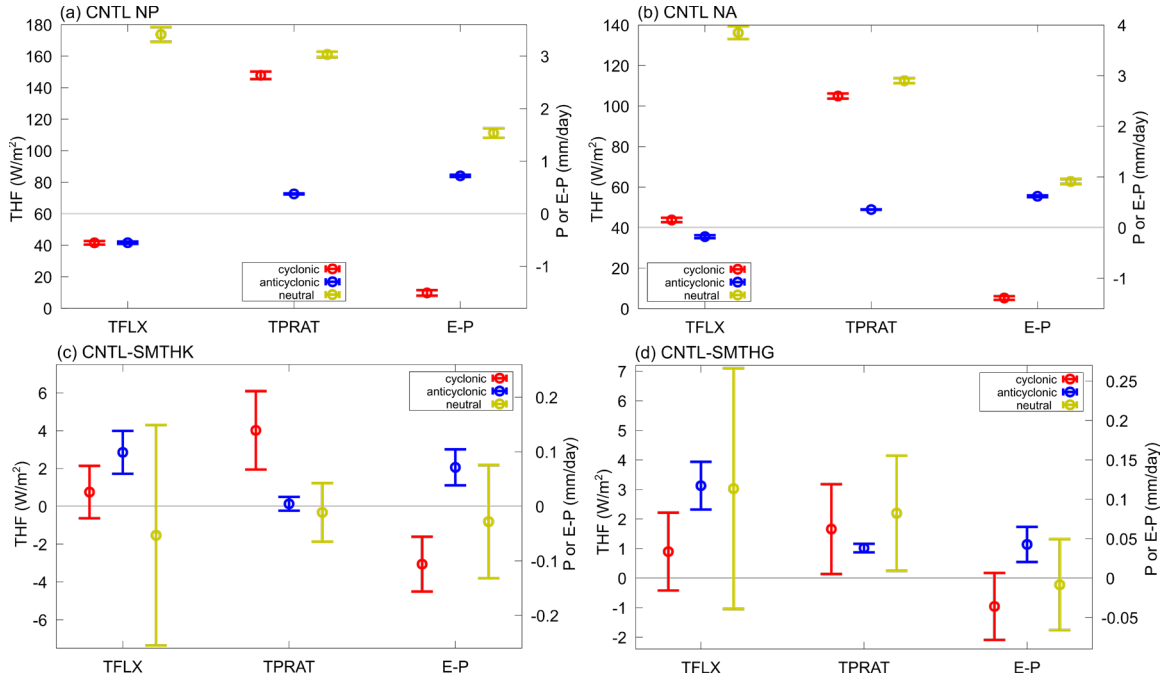

Figure S2. Same as in Fig. 3, respectively, but for the results based on a curvature threshold of $\pm 1.0 \times 10^{-6}$ m^{-1}, corresponding to a curvature radius of 1,000km.
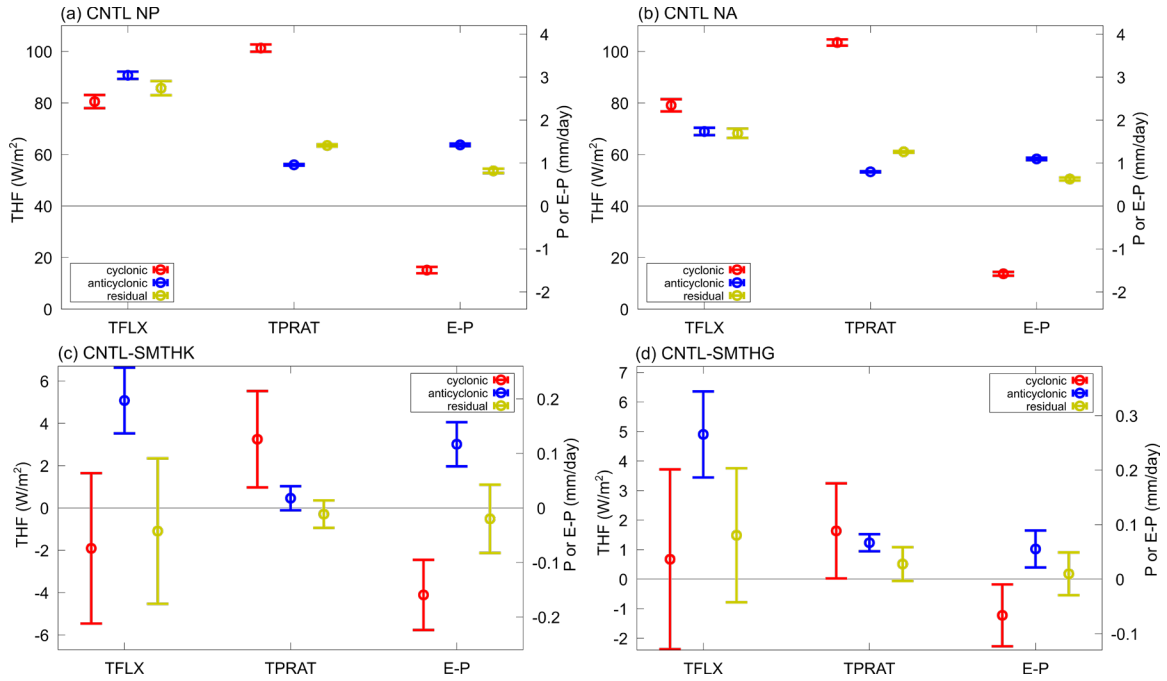
Figure S3. Same as in Fig. 3, respectively, but for the results based on the curvature of 925-hPa winds.
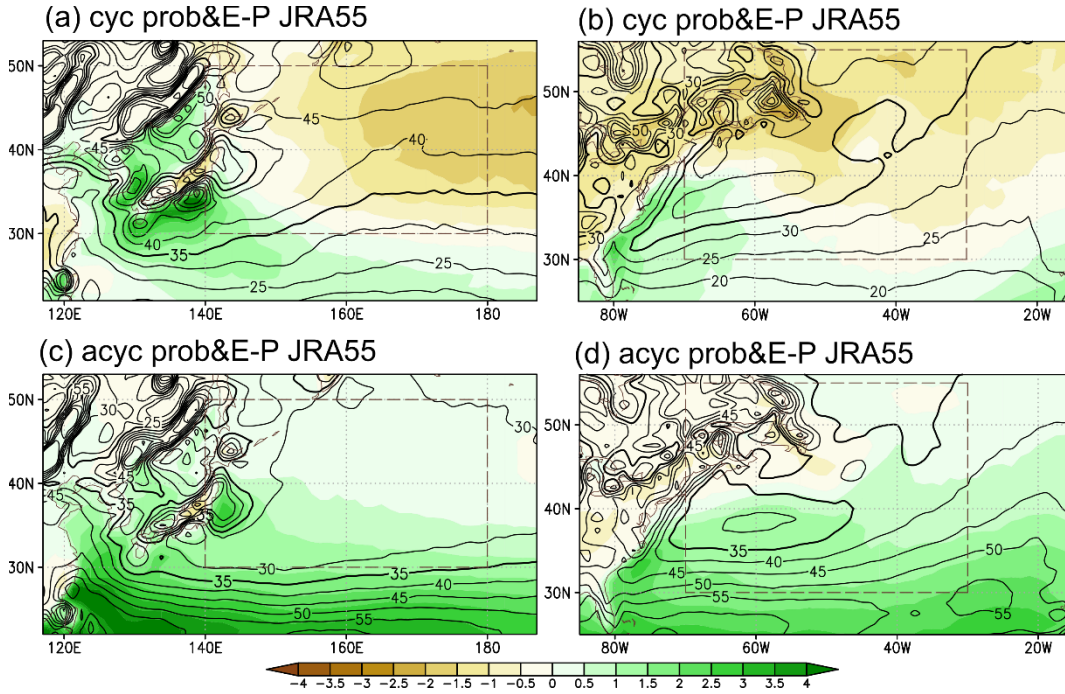

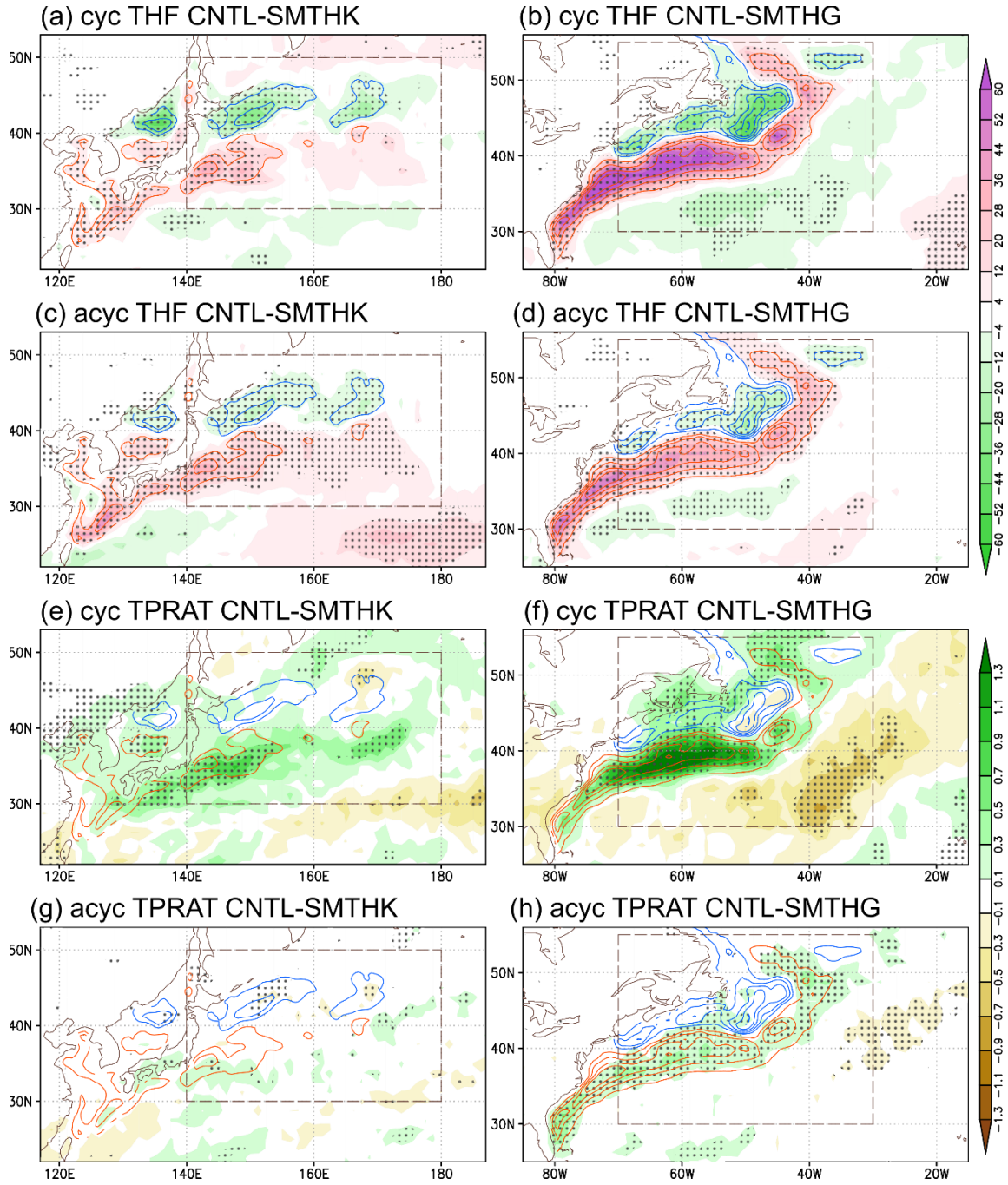**Figure S4.** Same as in Figs. 1c-f, respectively, but for the results based on the JRA-55 reanalysis.

Figure S5. a-b Difference in climatological-mean wintertime net turbulent heat flux (black contours, W/m²) between CNTL and SMTHK (CNTL−SMTHK) for (a) cyclonic and (b) anticyclonic contributions. Stipples denote statistically significant signals at 90% confidence level by Student's *t*-test. Red and blue contours indicate regions of warmer and colder SST (every 1K, zero contour omitted) in CNTL compared to SMTHK. **c-d** As panels a-b, respectively, but for total precipitation (mm/day). **e-h** As panels a-d, respectively, but for the differences between CNTL and SMTHG (CNTL−SMTHG). Dashed boxes signify the domains used to calculate the area-averaged contributions for the NP and NA, respectively.
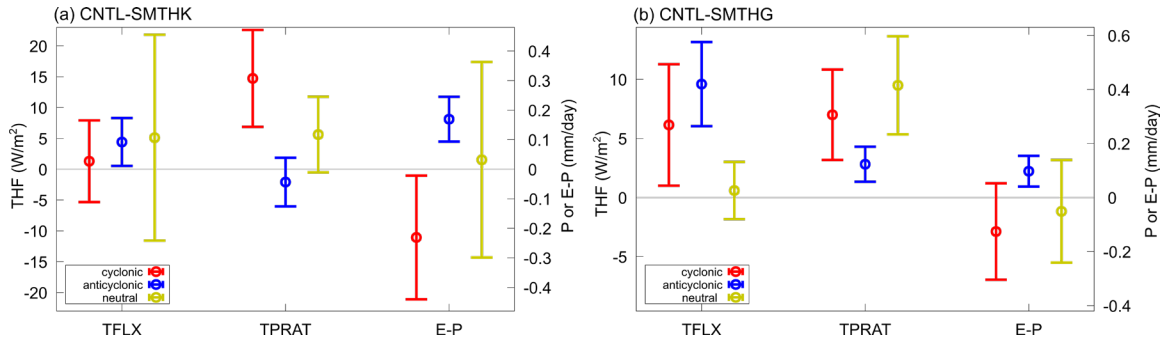
Figure S6. Same as in Figs. 3a-b, respectively, but for the results based on the JRA-55 reanalysis.
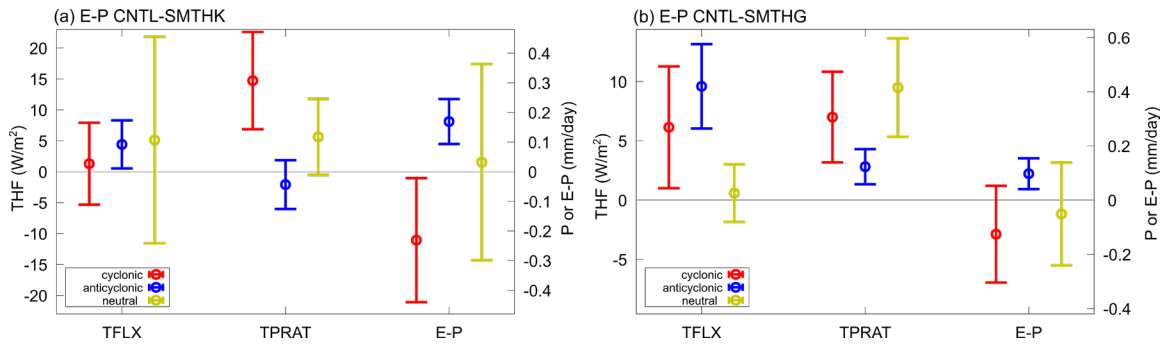

Figure S7. Same as in Fig. 3c-d, respectively, but for the results normalized by the corresponding probabilities of domains at 850-hPa for individual seasons.
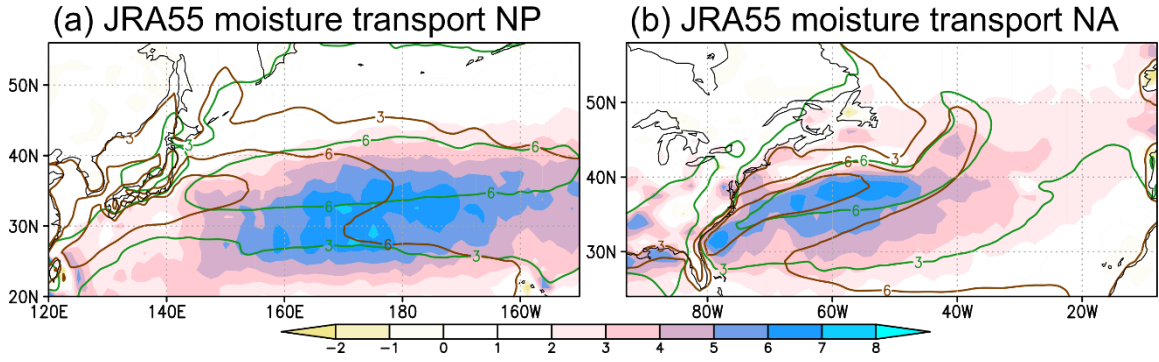
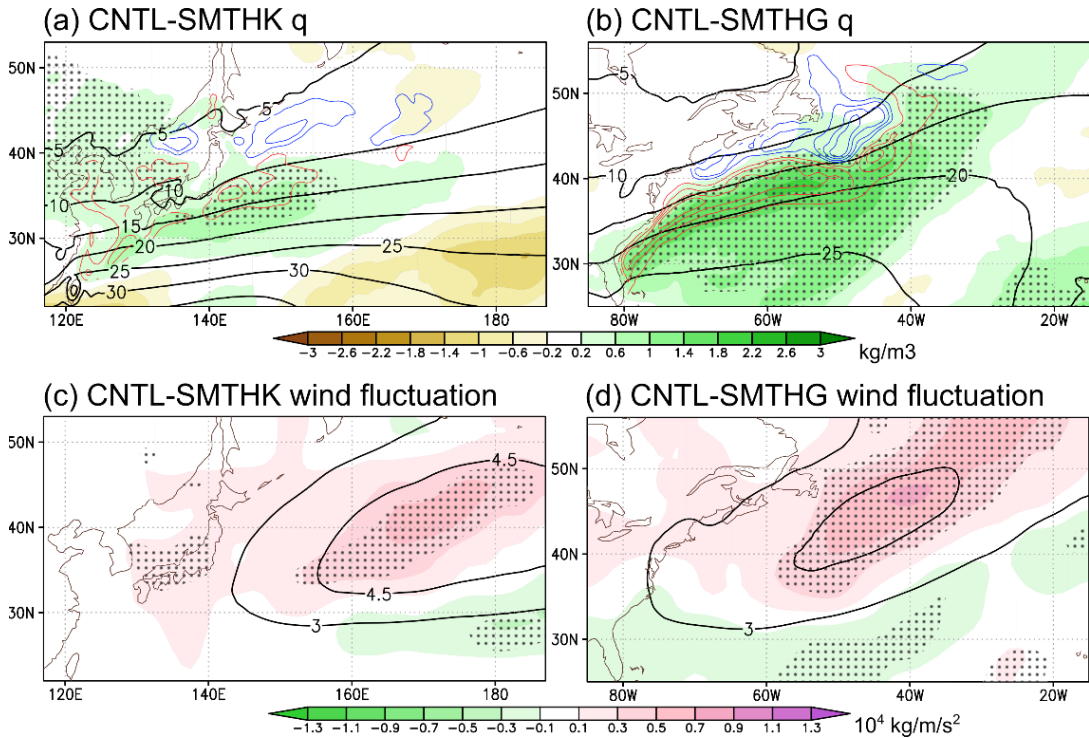**Figure S8.** Same as in Figs. 4a-b, respectively, but for the results based on the JRA-55 reanalysis.

Figure S9. a Total response (CNTL−SMTHK) of the climatological specific humidity (shadings in kg/m^3) integrated vertically from the surface to 100-hPa. Stipples signify statistically significant signals at 90% confidence levels by Student's *t*-test. Contours denote vertically-integrated climatological specific humidity (kg/m^3) in CNTL. **b** Same as in (a), but for the total response of CNTL−SMTHG. **c-d** Same as in a-b, but for the variance of high-pass-filtered wind fluctuation projected onto the upgradient direction of local curvature (shadings in 10^4 kg/m/s^2; see Text S2 for details) integrated vertically from the surface to 700-hPa. In a-b, red and blue contours indicate regions of warmer and colder SST (every 1K, zero contour omitted) in CNTL compared to SMTHK or SMTHG.